

Asymmetric Partitioning of Anions in Lysozyme Dispersions

Pierandrea Lo Nostro,^{*,†} Niccolò Peruzzi,[†] Mirko Severi,[†] Barry W. Ninham,^{†,‡} and Piero Baglioni[†]

Department of Chemistry and CSGI, University of Florence, 50019 Sesto Fiorentino, Florence, Italy, and Department of Applied Mathematics, Research School of Physical Sciences and Engineering, Institute of Advanced Studies, Australian National University, Canberra, Australia 0200

Received March 4, 2010; E-mail: pln@csgi.unifi.it

Abstract: An aqueous dispersion of lysozyme and sodium dodecyl sulfate phase separates below the cloud point. Two liquid phases are formed. At $\text{pH} < \text{pI}$ electrolytes change the cloud point temperatures (T_c). These follow an inverse Hofmeister series. Anions partition asymmetrically between the two phases. At fixed cation, the partitioning depends on the specific anion. In a system of finite volume, a concentrated dispersion of a protein is able to act as a chemical "sponge". No active pump is necessary to maintain concentration differences between concentrated and dilute dispersions.

Introduction

Electrolytes and neutral cosolutes modify the phase behavior and function of proteins. To what extent depends on their nature, concentration, pH, and ion pair specificity. Specific ion or Hofmeister effects are not accounted for by classical theories of electrolytes or colloids.^{1–3} The first studies of Hofmeister reported the different effectiveness of electrolytes in stabilizing aqueous protein dispersions.¹ The Hofmeister sequence, a particular ordering of effectiveness of salts in precipitating the peptide, occurred. Chaotropic, weakly hydrated ions such as iodide or thiocyanate promote the unfolding and solubilization of the polypeptide, while kosmotropic, strongly hydrated species such as fluoride or sulfate stabilize and salt-out the protein in its folded structure.⁴ The sequence is not unique. Changing the pH or substrate (below or above the protein pI) often produces a reversal in the sequence. The most studied protein, Hofmeister's choice, is hen egg white lysozyme.^{5–13} Its cloud point temperature (T_c) shows significant specific ion effects. Below T_c there is a protein-rich lower phase, in equilibrium with an upper, protein-poor layer.¹⁴ Classical electrolyte theories cannot account for the effects. The inclusion of quantum mechanical dispersion forces that depend on specific ionic polarizabilities, substrate dielectric properties, and their electromagnetic fre-

quency dependence is necessary.^{15,16} Such ion specificity always occurs at moderate (physiological) and high concentrations. They can even occur at low concentrations.^{17,18}

The matter goes beyond interactions. The same quantum mechanical forces conspire together with electrostatics and ion size to determine also the hydration of ions and free energies of adsorption and transfer.^{19,20} The specific effects of ions are not limited to aggregation, stability (folding/unfolding), and structural features of proteins alone. They are important in changing their functional features (e.g., coagulation cascade).^{21,22} Further the role played by active specific ion pumps embedded in biomembranes is crucial to the function of cells. Active pumps maintain the required concentrations of specific ions inside and outside the cytoplasm.

Ions bind at biological interfaces such as proteins and lipids.^{11,23,24} Several studies have addressed this issue. Among them, Tatulian reported on the binding constant of some cations and anions on phospholipid bilayers.²³ He observed that, besides specific binding sites for cations or for anions, the lipid aggregates possessed also common ion binding sites for both

[†] University of Florence.

[‡] Australian National University.

- (1) Kunz, W.; Lo Nostro, P.; Ninham, B. W. *Curr. Opin. Colloid Interface Sci.* **2004**, *8*, 1–18.
- (2) Boström, M.; Williams, D. R. M.; Ninham, B. W. *Phys. Rev. Lett.* **2001**, *87*, 168103–1/4.
- (3) Curtis, R. A.; Steinbrecher, C.; Heinemann, M.; Blanck, H. W.; Prausnitz, J. M. *Biophys. Chem.* **2002**, *98*, 249–265.
- (4) Zhang, Y.; Cremer, P. S. *Proc. Natl. Acad. Sci. U.S.A.* **2009**, *106*, 15249–15253.
- (5) Broide, M. L.; Tominc, T. M.; Saxowsky, M. D. *Phys. Rev. E* **1996**, *53*, 6325–6335.
- (6) Wentzel, N.; Gunton, J. D. *J. Phys. Chem. B* **2007**, *111*, 1478–1481.
- (7) Ishimoto, C.; Tanaka, T. *Phys. Rev. Lett.* **1997**, *39*, 474–477.
- (8) Taratuta, V. G.; Holschbach, A.; Thurston, G. M.; Blankschein, D.; Benedek, G. B. *J. Phys. Chem.* **1990**, *94*, 2140–2144.
- (9) Grigsby, J. J.; Blanch, H. W.; Prausnitz, J. M. *Biophys. Chem.* **2001**, *91*, 231–243.

- (10) Muschol, M.; Rosenberger, F. *J. Chem. Phys.* **1997**, *107*, 1953–1962.
- (11) Riès-Kautt, M. M.; Ducruix, A. F. *J. Biol. Chem.* **1989**, *264*, 745–748.
- (12) Riès-Kautt, M. M.; Ducruix, A. F. *J. Cryst. Growth* **1991**, *110*, 20–25.
- (13) Riès-Kautt, M. M.; Ducruix, A. F. *Method Enzymol.* **1997**, *276*, 23–59.
- (14) Curtis, R. A.; Lue, L. *Chem. Eng. Sci.* **2006**, *61*, 907–923.
- (15) Parsons, D. F.; Ninham, B. W. *Langmuir* **2010**, *26*, 1816–1823.
- (16) Ninham, B. W.; Lo Nostro, P. *Molecular Forces and Self Assembly: In Colloid, Nano Sciences and Biology*; Cambridge University Press: Cambridge, 2010.
- (17) Salis, A.; Boström, M.; Medda, L.; Parsons, D. F.; Barse, B.; Monduzzi, M.; Ninham, B. W. *Langmuir* **2010**, *26*, 2484–2490.
- (18) Ninham, B. W.; Yaminsky, V. *Langmuir* **1997**, *13*, 2097–2108.
- (19) Parsons, D. F.; Ninham, B. W. *J. Phys. Chem. A* **2009**, *113*, 1141–1150.
- (20) Boström, M.; Ninham, B. W. *J. Phys. Chem. B* **2004**, *108*, 12593–12595.
- (21) Di Stasio, E. *Biophys. Chem.* **2004**, *112*, 245–252.
- (22) Jaenicke, R. *J. Biotechnol.* **2000**, *79*, 193–203.
- (23) Tatulian, S. A. *Eur. J. Biochem.* **1987**, *170*, 413–420.
- (24) Baldwin, R. *Biophys. J.* **1996**, *71*, 2056–2063.

cations and anions “depending on the relative polarizability, the fine structure of the electronic shell, geometrical features and other properties”.

Consequences of Ion Binding in Finite Volume Two-Phase Systems. In this paper we address an extraordinary consequence of the specificity of ion binding suggested in ref 25. The phenomenon is of interest for separation technologies generally where Hofmeister effects have not been systematically exploited. It is interesting too for another reason. It implies that active ion pump mediated transport across membranes may not be the sole mechanism by which a cell maintains the concentration gradient between the intracellular cytoplasm and the extracellular matrix. The chemical sponge must contribute to the maintenance of such ionic partitioning.

While it is accepted that ion pumps are driven by biochemical mechanisms,²⁶ we have shown previously in a different model system that ion partitioning can be achieved also without the presence of such active ion carriers. Such a model proof-of-concept system was provided by phase separated aqueous dispersions of a short chain phospholipid (dioctanoyl-phosphatidylcholine, diC₈PC). In this system an asymmetric distribution of the ions occurs in a finite volume that contains the two phases in equilibrium. The partitioning ratio depends on the nature of the added electrolyte.^{27,28}

For the diC₈PC dispersion, ions interact with a homogeneous smooth surface of self-assembled rods, made up of an inner core occupied by the hydrocarbon tails of the phospholipid and surrounded by the zwitterionic headgroups.^{27,28} The ion specific finite volume partitioning effect provides a prototype effective ion pump.

Here we take this hint of an additional contribution to real (biological) ion pumps further. We tested the partitioning of electrolytes induced by a more realistic biological probe. Several sodium salts were used to study their effects on the cloud point temperature and the asymmetric partitioning of ions between the two separated phases of a surfactant/protein complex. The system comprises lysozyme and sodium dodecyl sulfate (SDS) at pH 10.2. The cloud point results follow a reverse Hofmeister series.^{4,17,29}

This reflects the increasing adsorption of the ions at the protein interface depending on their polarizability, and that results in stronger intermolecular interactions between lysozyme molecules. The ion partitioning between the two phases is asymmetric. Among the investigated anions, bromide largely accumulates in the lower, protein-rich layer. We discuss the results in terms of excluded volume, unfolding, specific binding sites, and protein surface features.

Results and Discussion

The conditions used were pH = 10.2, HCO₃⁻/CO₃²⁻ buffer concentration 25 mM, lysozyme:SDS mole ratio 1:87, and total concentration of lysozyme and SDS 7.5% w/w; the protein forms a stable complex with the anionic surfactant. This system has been studied for a long time at varying pH, composition, and

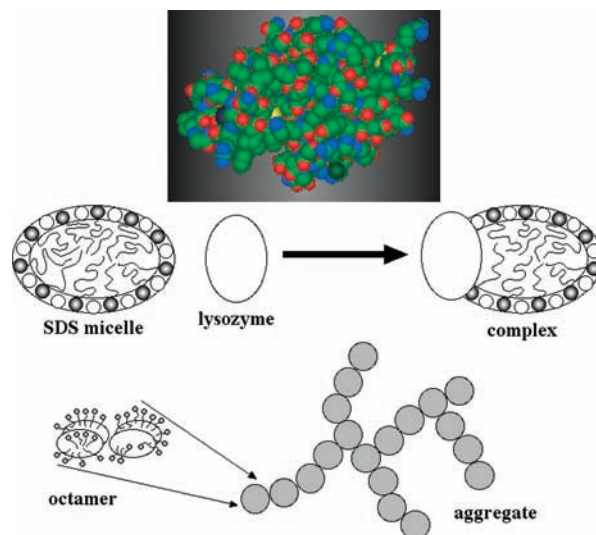


Figure 1. Top: molecular model for lysozyme (from 1Z55 PDB file). Center: schematic structure of an SDS micelle and of its complex with lysozyme. Empty circles represent the Na⁺ counterions of SDS. Bottom: schematic structure of an octamer and its aggregation in fibrils. Adapted from refs 35 and 38.

ionic strength.^{30–35} It is probably the most studied Hofmeister system. Earlier studies proposed various models for the complex.^{36,37} More recently it was proposed that in the complex one single protein molecule joins a single SDS micelle; cf. Figure 1.³⁵

In the complex a molecule of the protein is associated with a micelle of SDS, whose size and aggregation number ($N_{\text{agg}} = 87$) are similar to those of a regular SDS micelle ($14.7 \times 23.4 \times 23.4 \text{ \AA}^3$, $N_{\text{agg}} = 96$, at 25 °C).³⁹ The hydrodynamic radius of the lysozyme–SDS complex is $\sim 26 \text{ \AA}$ at pH 9.⁴⁰ Lysozyme itself is a compact globular protein, a nearly spherical prolate ellipsoid ($a = 27.5 \text{ \AA}$ and $b = 16.5 \text{ \AA}$),⁴¹ with a pI of ~ 11 and a molecular mass of $\sim 14\,600 \text{ Da}$. The pI is 11.35 in 0.1 M salt.⁴² The interior of the protein is strongly hydrophobic, and the surface coated by both charged residues and apolar patches (aromatic side groups).³³ At pH 10.2 it possesses a net charge of $+7e$.³² Since the properties of a macromolecule depend on its environment, a modification of background electrolyte (type and/or concentration) as well as choice of buffer can lead to significant variation of its structural features (conformations) and distribution of surface charges (isoelectric point). In the complex with SDS, the protein retains its compact structure almost unaltered in its folded state. Therefore, the complex can

(25) Ninham, B. W.; Boström, M. *Cell. Mol. Biol.* **2005**, *51*, 803–813.

(26) Hilgemann, D. W. *Annu. Rev. Physiol.* **1997**, *59*, 193–220.

(27) Lagi, M.; Lo Nostro, P.; Fratini, E.; Ninham, B. W.; Baglioni, P. *J. Phys. Chem. B* **2007**, *111*, 589–597.

(28) Boström, M.; Lima, E. R. A.; Biscaia, E. C., Jr.; Tavares, F. W.; Lo Nostro, P.; Parsons, D. F.; Deniz, V.; Ninham, B. W. *J. Phys. Chem. B* **2009**, *113*, 8124–8127.

(29) Boström, M.; Tavares, F. W.; Finet, S.; Skouri-Panet, F.; Tardieu, A.; Ninham, B. W. *Biophys. Chem.* **2005**, *117*, 217–224.

(30) Morén, A. K.; Khan, A. *Langmuir* **1995**, *11*, 3636–3643.

(31) Morén, A. K.; Khan, A. *Langmuir* **1998**, *14*, 6818–6826.

(32) Narayanan, J.; Deotare, V. W. *Phys. Rev. E* **1999**, *60*, 4597–4603.

(33) Stenstam, A.; Khan, A.; Wennerström, H. *Langmuir* **2001**, *17*, 7513–7520.

(34) Stenstam, A.; Khan, A.; Wennerström, H. *Langmuir* **2004**, *20*, 7760–7765.

(35) Narayanan, J.; Rasheed, A. S. A.; Bellare, J. R. *J. Colloid Interface Sci.* **2008**, *328*, 67–72, and references therein.

(36) Reynolds, J. A.; Tanford, C. *J. Biol. Chem.* **1970**, *245*, 5161–5165.

(37) Shirahama, K.; Tsujii, K.; Takagi, T. *J. Biochem.* **1974**, *75*, 309–319.

(38) Stenstam, A.; Montalvo, G.; Grillo, I.; Grzelski, M. *J. Phys. Chem. B* **2003**, *107*, 12331–12338.

(39) Prévost, S.; Grzelski, M. *J. Colloid Interface Sci.* **2009**, *337*, 472–484.

(40) Valstar, A.; Brown, W.; Almgren, M. *Langmuir* **1999**, *15*, 2366–2374.

(41) Price, W. S.; Tsuchiya, F.; Arata, Y. *J. Am. Chem. Soc.* **1999**, *121*, 11503–11512.

(42) Gimel, J. C.; Brown, W. *J. Chem. Phys.* **1996**, *104*, 8112–8117.

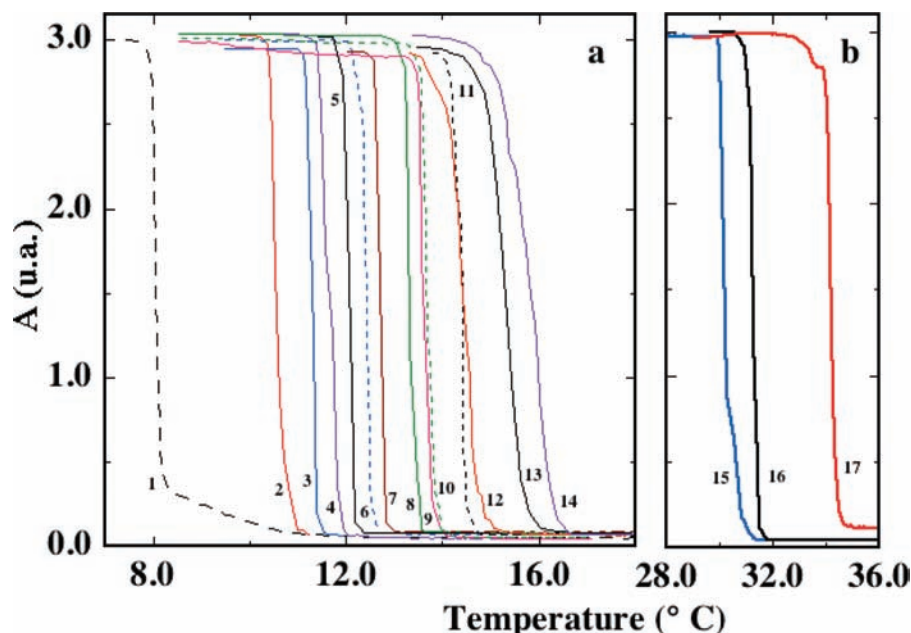


Figure 2. Turbidity profiles of lysozyme/SDS complexes in aqueous dispersions in the presence of different electrolytes (0.25 M). (1) salt-free, (2) NaF, (3) NaCl, (4) Na₂SO₄, (5) NaN₃, (6) NaBr, (7) NaNO₃, (8) Na₂SeO₄, (9) HCOONa, (10) CH₃COONa, (11) NaI, (12) NaOCN, (13) NaClO₄, (14) NaSCN, (15) KCl, (16) KSCN, (17) KSeCN.

be visualized as a swollen micelle with the protein lying near the micellar shell.^{31,43} On cooling, the suspension of lysozyme/SDS complexes first forms aggregates. These are made up of octamers of protein surrounded by the anionic surfactant chains. In time, the aggregates evolve and form amyloid-like fibrils (see Figure 1).³⁸ The existence of such high order aggregates is confirmed in concentrated dispersions of the protein, without surfactants, in the presence of salts through PGSE NMR experiments.⁴¹ The aggregation of the protein seems to proceed by progressive growth of dimers, tetramers, and larger structures.⁴⁴ The factors that drive the lysozyme aggregation are temperature lowering, pH increment (close to the pI), and high salt concentration.^{45,46} The aggregation behaviors of the pure protein and of its complex with SDS are very similar. In summary the shape, structure, size, and aggregation properties of the lysozyme/SDS complex are quite similar to those of the pure protein, at least for an SDS/lysozyme mole ratio lower than 100.⁴⁷

Cloud Point. Figure 2a shows the turbidity profiles of lysozyme/SDS for water (curve 1) and 0.25 M sodium salt solutions. All salts increase the cloud point temperature T_c over that in pure water (see Table 1). This can be attributed to the interaction between anions and the protein's basic charged groups. This enhances the protein–protein van der Waals interactions, which results in a shift in the cloud point temperature.⁵ The sequence from left to right in the figure confirms a reversed Hofmeister series, as expected with $\text{pH} < \text{pI}$. We can infer that kosmotropic (strongly hydrated) anions produce the smallest increment in T_c .

Table 1. Cloud Point Temperature T_c (K), Anion's Partitioning Ratio $\ln([\text{Down}]/[\text{Up}])$, Molar Surface Tension Increment σ ($\text{mN}\cdot\text{L}/\text{m}\cdot\text{mol}$),^{1,49,67} and Partial Molar Volume v_s (cm^3/mol) at 20 °C for the Different Salts in 0.25 M Aqueous Solution⁶⁸

anion	T_c	$\ln([\text{down}]/[\text{up}])$	σ	v_s
(water)	283.0	—	—	—
NaF	283.8	0.26	2.0	−1.21
AcONa	286.8	—	0.9	41.15
NaCl	284.4	0.37	1.6	17.71
NaBr	285.4	0.44	1.3	24.29
NaN ₃	286.1	—	—	25.77
NaNO ₃	285.9	0.14	1.1	28.91
NaI	287.5	−0.02	1.0	35.84
Na ₂ HPO ₄	283.0	—	—	9.33
Na ₂ SO ₄	284.7	—	1.7	19.51
HCOONa	286.8	—	—	—
Na ₂ SeO ₄	286.5	—	—	—
NaClO ₄	288.3	−0.22	0.6	45.80
NaSCN	288.6	−0.20	0.5	42.50
NaOCN	287.6	0.27	—	26.37
KSeCN	307.3	—	—	61.35
KCl	303.3	—	—	28.03
KSCN	304.4	—	—	51.05

Chaotrope (weakly hydrated) anions shift the onset of turbidity to the far right-hand side of the plot. Figure 2b illustrates the turbidity curves in the presence of KCl, KSCN, and KSeCN. It is interesting to note the sequence $\text{Cl}^- < \text{SCN}^- < \text{SeCN}^-$ that reflects the different polarizabilities of the anions. There is a significant specific cation effect when sodium is replaced by potassium. In fact KCl and KSCN increase T_c by ~ 17 °C with respect to NaCl and NaSCN. This effect can presumably be ascribed to the different interactions of potassium and sodium ions with the sulfate group of the SDS chains (the Krafft point of KDS is 34 °C, while that of SDS is between 8 and 12 °C).⁴⁸ In passing, we recall that in a recent paper it was

(43) Fukushima, K.; Murata, Y.; Nishikido, N.; Sugihara, G.; Tanaka, M. *Bull. Chem. Soc. Jpn.* **1981**, *54*, 3122–3127.

(44) Li, M.; Nadarajah, A.; Pusey, M. *J. Cryst. Growth* **1995**, *156*, 121–132.

(45) Ducruix, A.; Guilloteau, J. P.; Riès-Kautt, M.; Tardieu, A. *J. Cryst. Growth* **1996**, *168*, 28–39.

(46) Giordano, R.; Wanderlingh, F.; Wanderlingh, U.; Teixeira, J. *J. Phys. IV* **1993**, *3*, 237–240.

(47) Lad, M. D.; Ledger, V. M.; Briggs, B.; Green, R. J.; Frazier, R. A. *Langmuir* **2003**, *19*, 5098–5103.

(48) Paula, S.; Sus, W.; Tuchtenhagen, J.; Blame, A. *J. Phys. Chem.* **1995**, *99*, 11742–11751.

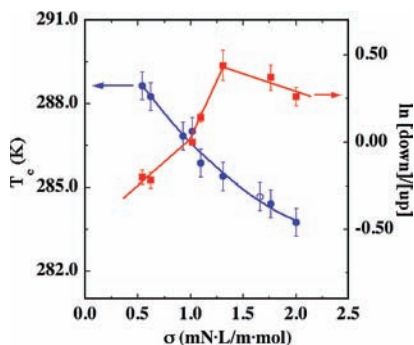


Figure 3. Cloud point temperature (blue) and partitioning coefficient (red) as a function of the molar surface tension increment of the anion. Full circles are for monovalent anions; the open circle is for SO_4^{2-} .

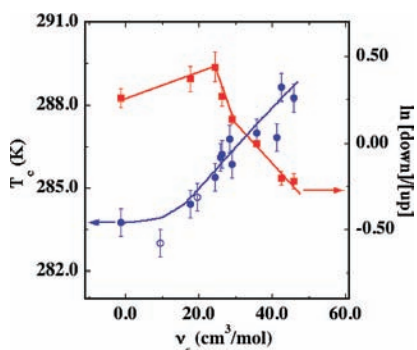


Figure 4. Cloud point temperature (blue) and partitioning coefficient (red) as a function of the partial molar volume of the anion. Full circles are for monovalent anions; open circles are for HPO_4^{2-} and SO_4^{2-} .

shown that the surface charge density of mesoporous silica strongly depends on the cation.¹⁷

To our knowledge this is the first work where the effect of selenocyanate is reported in the framework of a Hofmeister study. It shows that, in the homologous series of isoelectronic anions (N_3^- , OCN^- , SCN^- , SeCN^-), SeCN^- has the most chaotropic behavior. This might be expected in view of its size. The question of “ion size” is a vexed one that depends on dispersion forces also. It is both ion and ion pair specific. Ion size can be chosen to include hydration, and this is certainly necessary to accommodate bulk activities. Differences in hydrated radii and corresponding assumed hard core radii can compensate for specific ion effects as they determine interactions.^{15–19}

The anion effect on T_c is correlated with the molar surface tension increment (σ , see Figure 3, blue curve). This suggests that the main mechanism that drives the overall effect of electrolytes on the liquid–liquid phase separation is the anionic adsorption at the water/protein interface.⁴⁹

Figure 4 depicts the correlations between T_c and v_s (partial molar volume) of the electrolytes. This probably reflects the fact that T_c increases with the size of the anion. The value of v_s for sodium azide, sodium cyanate, and potassium selenocyanate was measured through the density of aqueous solutions at different concentrations (see Supporting Information). All values for sodium salts fall on the same curve within the experimental error.

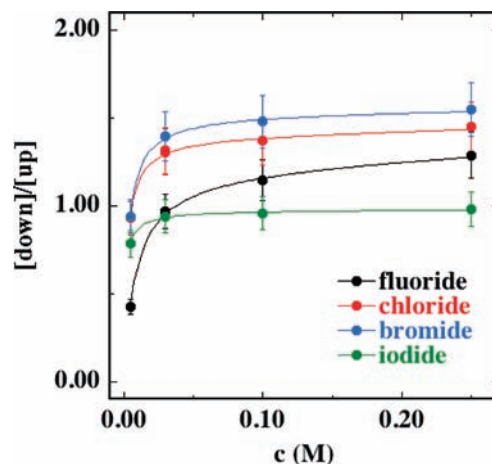


Figure 5. Partitioning ratio $[\text{down}]/[\text{up}]$ as a function of the salt concentration for NaF (black), NaCl (red), NaBr (blue), and NaI (green). The data are fitted with a modified Langmuir isotherm equation (eq 1).

The two exceptions are acetate and the divalent monohydrogenphosphate, presumably because of their hydrolysis.

Anion Partitioning. Figures 3 and 4 show the variation of the partitioning coefficient expressed as $\ln([\text{down}]/[\text{up}])$ as a function of σ and v_s , respectively. In the case of F^- , Cl^- , and Br^- the anion progressively accumulates in the lower phase following the trend of the polarizability ($\text{F}^- < \text{Cl}^- < \text{Br}^-$) or of the surface tension increment σ ($\text{F}^- > \text{Cl}^- > \text{Br}^-$), suggesting that ion adsorption is the main mechanism. However for anions larger than Br^- , the trend is not regular and there is no evident correlation between the partitioning ratio and σ . This means that the mechanism that dominates the distribution of the anion between the two phases cannot be simply described in terms of ion adsorption at the protein interface. Instead, Figure 4 seems to suggest that the partial molar volume (v_s) is a key factor in this process. In the plot of the partitioning ratio versus v_s the data show a maximum in the partitioning ratio corresponding to bromide; all other anions produce a less pronounced difference in ion concentration between the two phases. If anion adsorption were the driving force for the accumulation of the ion in the lower, protein-rich phase, we should have found a regular increasing trend in the $\ln([\text{down}]/[\text{up}])$ versus v_s plot. This was actually the case for a similar experiment carried out on the short chain phospholipid diC_8PC .²⁷

Figure 5 shows the partitioning ratio $[\text{down}]/[\text{up}]$ for the halides as a function of the salt concentration, between 5 and 250 mM. At all concentrations, the partitioning sequence is $\text{Br}^- > \text{Cl}^- > \text{F}^- > \text{I}^-$. Apparently, iodide partitions evenly between the two phases, while the other anions accumulate in the lower, protein-rich layer.

To analyze the results, we fitted the data with a Langmuir isotherm plus a linear term. The addition of the linear term accounts for the specific ion effects on the interfacial tension at the protein/water interface.⁴

$$\frac{[\text{down}]}{[\text{up}]} = \frac{B_{\text{sat}} K_A [c]}{1 + K_A [c]} + b [c] \quad (1)$$

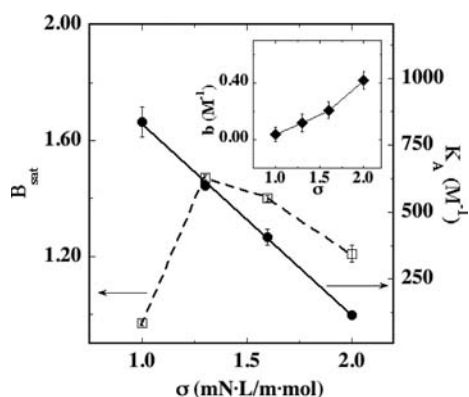
Here $[c]$ is the initial concentration of the electrolyte, K_A is the apparent equilibrium constant for the anion binding to the complex, B_{sat} is the saturation value attained by the partitioning ratio, and b is the first-order coefficient that is directly related to the hydration properties of the ion (e.g., entropy change of

(49) Boström, M.; Williams, D. R. M.; Ninham, B. W. *Langmuir* **2001**, *17*, 4475–4478.

Table 2. Partitioning Ratio [Down]/[Up] ($\pm 10\%$) for Fluoride, Chloride, Bromide, and Iodide Starting from Different Concentrations (c , mol·L⁻¹) of Sodium Salt^a

anion	c	[down]/[up]	B_{sat}	K_A	b
fluoride	0.005	0.43	1.2 ± 0.1	116 ± 10	0.42 ± 0.15
	0.030	0.97			
	0.100	1.15			
	0.250	1.29			
chloride	0.005	0.93	1.4 ± 0.1	407 ± 30	0.21 ± 0.10
	0.030	1.31			
	0.100	1.37			
	0.250	1.45			
bromide	0.005	0.94	1.5 ± 0.1	607 ± 20	0.12 ± 0.09
	0.030	1.40			
	0.100	1.48			
	0.250	1.55			
iodide	0.005	0.78	0.97 ± 0.01	837 ± 60	0.04 ± 0.02
	0.030	0.94			
	0.100	0.96			
	0.250	0.98			

^a Parameters extracted from fitting the data according to eq 1.

**Figure 6.** B_{sat} (empty squares) and K_A (full circles) fitting coefficients as a function of the molar surface tension increment of the anion (σ). Inset: variation of b as a function of σ .

hydration and surface tension increment).⁵⁰ In a similar study, Cremer proposed to add an exponential term in the modified Langmuir isotherm to account for electrostatic interactions.⁴ However in the present study, since the pH (10.2) is quite close to the protein pI (11.35), and the salt concentration is large (0.25 M), we can reasonably neglect the contribution due to electrostatic interactions.

The values of B_{sat} , K_A , and b are shown in Table 2. Interestingly, the value of K_A varies regularly with the molar surface tension increment of the anion (σ), suggesting that the ion adsorption at the complex interface is increasingly favored as the chaotropic nature of the anion increases (see Figure 6). Instead, the value of B_{sat} reflects the partitioning ratio of each anion at saturation, i.e. for high salt concentration. The plot of B_{sat} versus σ shows the same maximum detected in Figures 3 and 4, corresponding to bromide. As pointed out by Cremer, the value of B_{sat} is critically correlated with the anion size.⁵¹

Our results confirm that the anion partitioning is controlled by the surface tension increment (or polarizability) of the ion, but the ion volume, the presence of specific binding sites for the ions, and the formation of aggregates between complex units

result in the reduction of the ion concentration that accumulates in the protein-rich phase. The following discussion is an attempt to explain this behavior.

To explain the results we have to take into account the nature and the structural features of lysozyme. Some of the different factors that seem to be involved in this process are the following:

1. *Solvent-Accessible Area and Interfacial Tension.* It was recently proposed that in its complex with SDS, lysozyme can adopt two basically different conformational states (folded and slightly unfolded).⁵⁵ Further, the formation of dimers and higher oligomers results in a decrease of the solvent-accessible surface area (ASA).⁵² The effect of ions on the solvent-accessible area has been discussed by Collins in the general framework of the mechanism that leads to salting in produced by chaotropes and salting out by kosmotropes on proteins.⁵² According to the Collins hypothesis, kosmotropes make water a poorer solvent for the protein. The opposite is supposed to occur with chaotropes. A consequence of such an effect is the reduction of the protein's ASA in the presence of kosmotropes and its increment with chaotropes. In a study on the kinetics of unfolding of chymopapain, López et al. have shown that chaotropes such as guanidinium chloride increase the ASA of the native protein more significantly than species with a more kosmotropic behavior (e.g., LiCl or Na₂SO₄).⁵³ However, the overall ASA change, which includes the variation in the polar and apolar solvent accessible surfaces, was relatively small, $\sim 10\%$. Moreover, the adsorption of chaotropic ions at the protein surface can contribute in changing the outer surface of the complex, by changing the relative contribution of α -helix, β -sheet, and random coil regions,⁴⁰ and therefore modify its hydration layer. Therefore we can expect that different salts may induce small changes in the protein surface area that is accessible to the solvent. Although a precise quantification of such a phenomenon is difficult to assess for the lysozyme/SDS complex system, in what follows we show that preliminary calculations can partially account for the observed results. In the framework of the model proposed by Curtis et al., the protein-protein interactions depend not only on several factors, e.g. solvation, hydrogen bonding, dispersion forces, but also on the solvent accessible surface area.³ The latter contribution is described in terms of a potential that is assumed to be proportional to the total area of the interacting protein molecules within a certain surface-to-surface separation approximated by the solvent diameter (D). If d is the diameter of a protein molecule, the potential is then written as $W(r) = -\chi A(r)$, where $A(r)$ is the buried surface area, given by the expression $A(r) = \pi d^2 - \pi dr + \pi Dd$ (for $d < r < D + d$), and χ is a scaling factor, directly related to the electrolyte background concentration. For $r = R + d$ the potential W falls to zero, and for $r = d$ it reaches the minimum value given by $-\pi\chi Dd$. The value of χ is unknown but, according to Curtis et al., is directly related to the surface tension molal increment (σ) of the ion. σ is small for large (chaotropic) ions and large for kosmotropic species; therefore it offsets the effect of D .³ As soon as the temperature of the lysozyme/SDS dispersion is lowered below the cloud point temperature, the complex units begin to aggregate and form the coacervate. In this process a significant reduction of the complex/water interfacial area occurs. The presence of chaotropic species (e.g., bromide, iodide, thiocyanate) enhances this phenomenon which reflects the low σ value of these ions. It is

(50) Zhang, Y.; Furyk, S.; Bergbreiter, D. E.; Cremer, P. S. *J. Am. Chem. Soc.* **2005**, *127*, 14505–14510.

(51) Cho, Y.; Zhang, Y.; Christensen, T.; Sagle, L. B.; Chilkoti, A.; Cremer, P. S. *J. Phys. Chem. B* **2008**, *112*, 13765–13771.

(52) Collins, K. D. *Methods* **2004**, *34*, 300–311.

(53) López-Arenas, L.; Solís-Mendiola, S.; Padilla-Zúñiga, J.; Hernández-Arana, A. *Biochim. Biophys. Acta* **2006**, *1764*, 1260–1267.

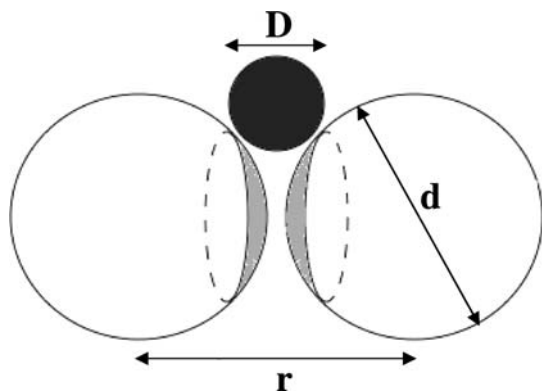


Figure 7. The two large spheres (diameter d) represent two protein molecules interacting at a distance r . The gray regions represent the buried area from which the solvent (black sphere, diameter D) is excluded. Adapted from ref 3.

important to recall that in fact electrolytes play their role at the protein–water and not at the air–water interface. Thus, we should not consider σ (obtained for air–water interfaces) but its corresponding σ_{pw} that reflects the variation of the protein–water interface upon addition of the salt.^{4,54} The value of σ_{pw} has been introduced and discussed more recently in the literature. While σ is always positive (small for chaotropes and large for kosmotropes), σ_{pw} can be positive or negative, depending on the protein and on the electrolyte. Although the trend is not regular, σ and σ_{pw} reach the maximum/minimum values for kosmotropes/chaotropes, reflecting the strong adsorption of large soft ions at the air–water and protein–water interfaces. In conclusion, the effects of the protein’s solvent accessible surface area and of the interfacial tension should lead to a stronger adsorption of the chaotropic anions at the complex–water interface and, therefore, to a more asymmetric ion partitioning between the two phases.

2. Excluded Volume. According to Schellman the interaction of an ion with a macromolecule is regulated by two opposing effects: the excluded volume and the specific binding.⁵⁵ The former limits the accumulation of ions at the surface, due to their hindrance, and the second should result in an increasing binding of some specific ions. The free energy cost (ΔG_{hydr}) necessary to dehydrate an ion when it adsorbs at the protein surface is lower for the big chaotropic species, and in fact these ions adsorb preferentially. However, as Figure 7 shows, the accumulation of ions at the protein surface is limited by their own size. We recall here the observation made by Cremer on the specific anion effect on the solution behavior of elastin-like polypeptides.⁵¹ The size of the anion was found to be the determinant for its adsorption at the biopolymer interface. In particular when studying the adsorption of the same anions on two different polymers that differ in hydrophobicity, it was found that anions larger than bromide partition preferably from the bulk aqueous solution to the less hydrophobic polymer surface, due to their limited accessibility to the binding sites in a more compact structure, i.e. that of a more hydrophobic macromolecule.

3. According to Collins’ law of matching water affinities, chaotropes are supposed to bind strongly to the basic residues of the protein (Lys and Arg), and form stable ion pairs.⁵² This

would explain the behavior of fluoride, chloride and bromide. These anions bind increasingly to the positive charges of the protein surface. However, it does not explain the behavior of anions larger than bromide. It is important to recall also the fact that ions and pH can modify the pK_a of basic aminoacids residues, as it was demonstrated by Ninham and by Ullmann.^{56,57} Such a change in turn can modify the surface potential of the protein, and eventually the intermolecular interaction between complex moieties, as well as the conformational and hydration states of the protein. Again, this process can alter the isoelectric point of the protein, depending on the nature and concentration of the electrolytes.

4. Typical chaotropes such as perchlorate, thiocyanate, nitrate, and iodide bind lysozyme at specific sites, rather than being randomly distributed on the protein surface.⁴ These sites can be protein specific, salt specific, or packing forbidden.⁵⁸ The strength of such interactions is so large that they determine the protein crystallization. As a matter of fact different anions induce polymorphism in lysozyme.⁵⁸ Although water molecules are probably involved in anion–protein interactions in the solution phase, it seems that no solvent is present in the crystal structures.⁴ This feature is relevant to our study. It has been demonstrated that in the case of Bacteriophage T4 lysozyme the interactions established in solution dictate those in the solid phase.⁵⁹ Once the anions are sandwiched between two protein molecules and form stable bridges, they favor protein–protein anisotropic interactions with a mechanism similar to the key-and-lock process typical of molecular recognition, where dispersion forces play the most prominent role.⁶⁰ Such interactions basically depend on the protein shape and surface roughness and determine the correct orientation of protein molecules before crystallization takes place.¹⁴ Finally, simulation studies performed by Jungwirth demonstrated that the adsorption of ion on a spherical particle is significantly influenced by the “patchy” surface of the protein, which exposes to the solvent both polar and hydrophobic regions, and the ion size.⁶¹ This is a more “chemical” effect as it strictly depends on the protein nature and on the specific ion that interacts with the macromolecule–water interface.

In conclusion, the cloud point and ion partitioning results seem to indicate that first ions interact with the lysozyme/SDS complex surface and adsorb more or less, depending on their chaotropic/kosmotropic nature. In this sense the most chaotropic species are supposed to strongly interact with the complex, lower the interfacial tension, and enhance the attractive interaction between different protein molecules. Once the macromolecular entities start forming oligomers and aggregate in fibrils, because of the reduction of the solvent exposed area and of excluded volume constraints, they necessarily desorb from the lower phase, and ions partition more evenly.

The above interpretation of the phenomena is couched in terms of conventional accepted language. We know this is inadequate in

(54) Dér, A.; Kelemen, L.; Fábrián, L.; Taneva, S. G.; Fodor, E.; Páli, T.; Cupane, A.; Cacace, M. G.; Ramsden, J. J. *J. Phys. Chem. B* **2007**, *111*, 5344–5350.

(55) Schellman, J. A. *Biophys. J.* **2003**, *85*, 108–125.

(56) Boström, M.; Williams, D. R. M.; Ninham, B. W. *Biophys. J.* **2003**, *85*, 686–694.

(57) Bombarda, E.; Ullmann, G. M. *J. Phys. Chem. B* **2010**, *114*, 1994–2003.

(58) Vaney, M. C.; Broutin, I.; Retailleau, P.; Douangamath, A.; Lafont, S.; Hamiaux, C.; Prangé, T.; Ducruix, A.; Riès-Kautt, M. *Acta Crystallogr.* **2001**, *D57*, 929–940.

(59) Chang, R. C.; Asthagiri, D.; Lenhoff, A. M. *Proteins* **2000**, *41*, 123–132.

(60) Neal, B. L.; Asthagiri, D.; Velev, O. D.; Lenhoff, A. M.; Kaler, E. W. *J. Cryst. Growth* **1999**, *196*, 377–387.

(61) Lund, M.; Jungwirth, P. *J. Phys.: Cond. Matter* **2008**, *26*, 494218.

light of ongoing developments. But it is a familiar language and hopefully captures the essence of what is going on.

While the role of dispersion forces is the key to specificity (both surface and bulk phenomena), much of the recent literature that quantifies them has relied on incomplete ionic polarizability data. The bringing to bear of *ab initio* techniques has now furnished new reliable data that makes prediction quantitative.^{15,16,19,62,63}

Frequency dependencies are not always what were expected. Further, the meaning of a measurement of pH itself depends on specific ion effects. It is a somewhat open matter, in biological systems especially, and above 0.1 M salt.^{16,64,65}

SDS Aggregation State. To check the aggregation state of SDS in the real dispersion, we proceeded in the following manner. The values of the CMC for SDS in the presence of electrolytes at different concentrations are available in the literature. From these, a plot of CMC versus the inverse of the Debye screening length, $\kappa_0 = \lambda_0^{-1}$ can be drawn. Then the value of κ_{eff} was calculated, according to eqs 2 and 3, considering the presence of the lysozyme molecules that act as a polyelectrolyte (with an overall charge +7). Once the real κ_{eff} is known, we can estimate the CMC of the surfactant in the system.⁶⁶

The values of the CMC of SDS at 298 K in the presence of NaCl were taken from the literature (see the Supporting Information).

$$\kappa_{\text{eff}} = \lambda_{\text{eff}}^{-1} = \kappa_0 \left[1 + \frac{\sqrt{1000N_A} \ln 3}{32\pi} \left(\frac{q^2}{\epsilon_0 \epsilon_r k_B T} \right)^{3/2} \times \frac{\left(\sum_{i=1}^n c_i z_i^4 \right) \left(\sum_{i=1}^n c_i z_i^2 \right) - \sum_{i=1}^{n-1} \sum_{j=i+1}^n c_i c_j z_i^2 z_j^2 (z_j - z_i)^2}{\left(\sum_{i=1}^n c_i z_i^2 \right)^{3/2}} \right] \quad (2)$$

where “*i*” and “*j*” are the different chemical species in the dispersion, i.e. lysozyme, Na⁺, dodecylsulfate ion, hydrogen-carbonate, carbonate, anion (from the added electrolyte), and OH⁻ (we neglected the concentration of H⁺ because of the overall alkaline environment imposed by the buffer). c_i and z_i represent the molar concentration and charge of each species “*i*”. N_A , q , ϵ_0 , ϵ_r , k_B , and T are the Avogadro number, elementary charge, vacuum permittivity, dielectric constant of water, Boltzmann constant, and absolute temperature, respectively. κ_0 is the inverse of the classical Debye screening length (λ_0) of the aqueous solution at temperature T , given by

$$\kappa_0 = \lambda_0^{-1} = \left(\frac{1000N_A q^2}{\epsilon_0 \epsilon_r k_B T} \sum_{i=1}^n c_i z_i^2 \right)^{1/2} \quad (3)$$

The values of λ_{eff} calculated with eq 2 span between 3.8 and 3.9 Å when the added electrolyte concentration ranges between 0.25 and 0.005 M. For these values of the Debye length, the CMC of SDS is ~ 0.53 mM (see Figure S1, Supporting Information). This result confirms that, even in the presence of lysozyme and added electrolytes (including the buffer ions), the surfactant is always in the micellar state, well above its CMC.

Conclusions

The cloud point temperature of the lysozyme/SDS complex at pH 10.2 in moderately high concentration depends on the nature of the added salt. A reversed Hofmeister series appears and suggests that specific nonelectrostatic ion–protein dispersion interactions dictate the process that leads to phase separation. Ions significantly modify the protein–protein interactions that in turn determine the behavior of highly concentrated protein dispersions, like those that exist in the cytoplasmatic environment, and play a central role in several diseases.⁵ The results parallel those obtained with different systems (e.g., zwitterionic surfactants) and reflect the different ion adsorption at the micellar or macromolecular interface, which is mainly ruled by the polarizability of the ions.

Once the two phases are separate, the anion concentration is quite asymmetric, indicating that the protein-rich phase can either accumulate or exclude most of the present ions. Here, more subtle different interdependent mechanisms are at work: polarizability and size of the ions, solvent-accessible surface area of the protein, folded/unfolded conformational states, specific binding sites, etc. No active metabolism is required to produce the different distribution of ions between the two coexisting phases; apparently a “simple” change in the aggregation state of the protein is sufficient to rule the ion partitioning.

In conclusion, whatever the mechanisms that dictate cloud point phenomena that are still to be unravelled in detail, the essential point we wish to make remains. In any such finite volume phase separated system, which can include the aggregated hemoglobin proteins in a red cell, specific ion binding exists. This leads to partitioning of competing ions. The competition for protein sites leads to a “chemical” sponge or an apparent ion pump. It is driven by dispersion forces missing from conventional theories that are limited to electrostatic forces alone.

The idea that a Donnan like equilibrium could provide an equilibrium mechanism for “ion pumps” goes back more than 50 years to the work of G. N. Ling.⁶⁹ The mechanism based on electrostatics alone failed. But once the operation of missing specific dispersion forces is recognized, the notion has more credibility.

How much of an effect this will have for real biological systems is open. The effects are nonetheless real.

Acknowledgment. The authors acknowledge the Consorzio Interuniversitario per lo Sviluppo dei Sistemi a Grande Interfase (CSGI, Florence) and the Ministero dell’Istruzione, dell’Università e della Ricerca (MIUR, Rome) for partial financial support.

Supporting Information Available: Details for the turbidity, phase separation, density, ion chromatography experiments, and aggregation state of SDS in the presence of salt at different concentrations. Values of density for aqueous solutions of potassium selenocyanate, sodium cyanate, and sodium azide at 20 °C, at four different salt concentrations. This material is available free of charge via the Internet at <http://pubs.acs.org>.

JA101603N

- (62) Parsons, D. F.; Ninham, B. W. *Langmuir* **2010**, Articles ASAP, DOI: 10.1021/la9041265.
- (63) Parsons, D. F.; Boström, M.; Maceina, T. J.; Salis, A.; Ninham, B. W. *Langmuir* **2010**, *26*, 3323–3328.
- (64) Evens, T. J.; Niedz, R. P. *Scholarly Res. Exch.* **2008**, 818461.
- (65) Salis, A.; Pinna, M. C.; Bilaničová, D.; Monduzzi, M.; Lo Nostro, P.; Ninham, B. W. *J. Phys. Chem. B* **2006**, *110*, 2949–2956.
- (66) Nylander, T.; Kékicheff, P.; Ninham, B. W. *J. Colloid Interface Sci.* **1994**, *164*, 136–150.
- (67) Henry, C. L.; Dalton, C. N.; Scruton, L.; Craig, V. S. J. *J. Phys. Chem. C* **2007**, *111*, 1015–1023.
- (68) Lo Nostro, P.; Fratoni, L.; Ninham, B. W.; Baglioni, P. *Biomacromolecules* **2002**, *3*, 1217–1224.
- (69) Ling, G. N.; Ochsenfeld, M. M. *J. Gen. Physiol.* **1966**, *49*, 819–843.